Available online at www.sciencedirect.com

ScienceDirect

journal homepage: www.elsevier.com/locate/he

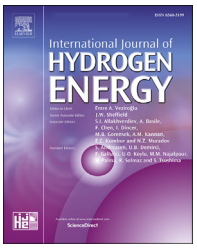

Density functional theory (DFT) calculations, synthesis and electronic properties of alkoxylated-chalcone additive in enhancing the performance of CMC-based solid biopolymer electrolyte

Wan M. Khairul [a,*], *Rafizah Rahamathullah* [b], *Janice Roria Joni* [a], *M.I.N. Isa* [c]

[a] *Faculty of Science and Marine Environment, Universiti Malaysia Terengganu, 21030, Kuala Nerus, Terengganu, Malaysia*

[b] *Faculty of Engineering Technology, Universiti Malaysia Perlis, Level 1, Block S2, UniCITI Alam Campus, Sungai Chuchuh, Padang Besar, 02100, Perlis, Malaysia*

[c] *Frontier of Materials Research Group, Advanced Materials Team, Ionic & Kinetic Materials Research (IKMaR) Laboratory, Faculty of Science and Technology, Universiti Sains Islam Malaysia, Bandar Baru Nilai, 71800, Nilai, Negeri Sembilan, Malaysia*

HIGHLIGHTS

- Anchoring alkoxylated chalcone as organic additive was designed, synthesized and assessed physico-chemically.
- Heptyloxy chain (-OC_7H_{15}) and nitro (-NO_2) substituents assisted majorly in the conductivity of SBE.
- New class of CMC-NH_4Cl-(Alkoxylated chalcone) SBE showed ionic conductivity up to 2.3×10^{-2} Scm^{-1}.

ARTICLE INFO

Article history:
Received 6 March 2022
Received in revised form
10 June 2022
Accepted 13 June 2022
Available online xxx

Keywords:
Chalcone-based dye
Additive
Ionic conductivity
Solid biopolymer electrolyte

ABSTRACT

Alkoxylated-chalcone having push-pull system has been integrated as additive in solid biopolymer electrolyte (SBE) based on carboxymethyl cellulose (CMC) doped with ammonium chloride (NH_4Cl). The structural, optical and thermal stability of the additive were characterized via FT-IR spectroscopy, UV–Vis, 1D NMR and TGA prior film casting as SBE. The optical band gaps (E_g^{opt}) of alkoxylated-chalcone additive exhibited low range, 3.14 eV which are comparable to that corresponding simulated findings, whereas they lie within the range of organic semiconductor materials. Frontier molecular orbitals (FMO) analysis, chemical reactivity and molecular electrostatic potential (MEP) revealed that the oxygen on alkoxy chain and $-NO_2$ substituent tuning the energy level of HOMO and LUMO. The investigation of their potential as additive in SBE system has been accomplished by incorporating CMC-NH_4Cl electrolyte using solution-casting method. A various weight ratio (0–8%) of additive was tested and doped with CMC-NH_4Cl as new SBE. The highest ionic conductivity achieved was 2.3×10^{-2} Scm^{-1} at ambient temperature (303K) for the system containing 8 wt.% of chalcone-based additive. The findings imply that the designated chalcone-based moiety has a potential to be employed as additive materials towards the performance enhancement for electrochemical the interests.

* *Corresponding author.*
E-mail address: wmkhairul@umt.edu.my (W.M. Khairul).

https://doi.org/10.1016/j.ijhydene.2022.06.125
0360-3199/

Please cite this article as: Khairul WM et al., Density functional theory (DFT) calculations, synthesis and electronic properties of alkoxylated-chalcone additive in enhancing the performance of CMC-based solid biopolymer electrolyte, International Journal of Hydrogen Energy, https://doi.org/10.1016/j.ijhydene.2022.06.125

Introduction

Nowadays, the fundamental investigation, progress and development of electrolyte materials have drawn intensive attention in various electrochemical devices and optoelectronic applications due to their vast advantages and benefits that they may offer in advanced materials studies [1–3]. Due to these motivations, in recent years an idea of adding an of small amount of additives on the electrolyte [4,5] becomes another promising alternative in influencing their performance and stability. Literally, research involving organic additive incorporating with renewable resource-based biopolymers are rather scarce, which the research incorporates the benefit of electronic properties arising from the designed molecules. To date, the interest is on making use the unique aspect of carbon-carbon bonds in the molecules to be integrated as additive in electrolyte to enhance carrier mobility and electrical performance at an optimum level. Many research works have implemented the use of small molecule dyes as additives on the polymer electrolyte that afford a variation of advantages to enhance the ionic conductivity, altering the structural stability of the electrolyte towards the enhancement of efficiency of electrochemical devices [6–9]. For instance, organic nitrogenous compound [10], pyridine [11], thioureas [12,13], carboxylic acid moiety [14] and thiophene [15] are some examples of organic compounds utilized as additives in polymer electrolyte (PE) to improve the efficiency of the dye-sensitized solar cell (DSSCs), supercapacitor and batteries application. Karthika et al. [12], have reported the conjugated hetero-organic pave the way for the architectural flow of electrons from them to the polymer and redox pair which helps in accumulating prosperous ionic conductivity and ion transport property in the devices. On top of that, Ganesan et al. [10], stated that the use of organic nitrogenous compounds in the polymer electrolyte also can lead to enhancement in polymer conductivities due to the donation of lone pairs of electrons.

In this sense, the selections of feasible functional groups also should have been given in depth attention in their roles and contributions toward conductivity which eventually would leave an effect toward the molecular conductance. Regarding to this matter, introduction of organic dye in polymer electrolyte as additives has become the simplest methods and promising alternative in enhancing the conductivity. As reported by Wang et al. [16], the presence of electron donating and hydroxyl end-group in additives assist the improvement of the conductivity. They demonstrated EDTA as additive to help in decreasing the crystallinity of polyvinylidene fluoride (PVDF). Ionic conductivity of the electrolyte composition can be improved effectively by the addition of chemical species or generically known as additive by reducing the crystalline phase of polymer, enhancing the salt dissolution and ion migration [17–19]. In this sense, by considering uniqueness of chalcone-based compound properties [20–22] such as having electronic delocalization in its extended π-orbital system, presence of carbonyl (C═O) and ethylene (C═C) moiety can contribute good charge transport to the polymer electrolyte system. Current studies had demonstrated that structural alteration in the core of chalcone-based moiety with substitution and sidechain can lead to the enhancement of electronic property, dielectric and electrochemical application [23–25]. Aligning with these motivations, with the interest of this report, we have introduced chalcone-type compound as additive in the composition of electrolyte which is hypothesised and predictable in allowing the two components in contact to each other hence creating an interaction with this electrolyte that resulted into enhancing the behaviour and properties of ionic electrical conductivity in this polymer electrolyte system.

Among various polymers electrolyte, solid polymer electrolytes (SPEs) are drawing extensive devotion as solid-state alternatives to liquid and crystalline electrolytes due to their advantages of desirable shape mouldability, light-weight, free from solvent leakage, biodegradable, low cost, non-toxic, high physical and chemical stability [26–29]. Nonetheless, SPEs which use of pure biopolymer materials as a polymer host have inherited some issues and disadvantages namely exhibiting low ionic conductivity at ambient temperature which may act as a barrier to their utility when compared with the existing conventional liquid and hybrid electrolytes [30,31]. In this context, low molecular weight organic solvents such as propylene carbonate (PC), glycerol, ethylene carbonate (EC), dimethyl carbonate (DMC), diethyl carbonate (DEC), polyethylene glycol (PEG), N,N−dimethylacetamide (DMAc), γ−butyrolactone and to name a few are several types of solvent additives that commonly used in plasticized polymer-salt electrolyte system [32–34]. For instance, Wong et al. [35], reviewed role and function of various additives which play a crucial role in enriching both the mechanical and electrical properties of polymer electrolyte membranes. Nevertheless, plasticization can result in deterioration in the mechanical integrity of the film and increased corrosive reactivity of polymer electrolyte because requires large amounts of plasticizers. There are also some limitations obtained such as slow evaporation, decreases in thermal, electrical and electrochemical stabilities.

Herein, the focus in this present study is to examine and evaluate how far the effects of organic dye additive dosage could be able to enhance the ionic conductivity of biopolymer-salt electrolyte system at room temperature. With the existence of strong inductive electron-withdrawing and electron donating group in the chalcone-based system are predictable to interact with biopolymer-salt electrolyte and consequently give alternative pathway for the electron flow to SBEs system. In this respect, the presence of heptyloxy chain ($-OC_7H_{15}$) as donor group and active nitro ($-NO_2$) functional group as acceptor in chalcone-based additive assist the enhancement of the ionic performance of the solid electrolyte. The blending modification approach is used to introduce functional groups into main chains of the biopolymer matrix to increase the mobility of carriers, improves salt solvating power which leads to the enhancement of ionic conductivity of the SBE.

Experimental

Materials and characterization

All chemicals, reagents and solvents were acquired from Sigma-Aldrich, Acrós Organics and Merck and were used as

Please cite this article as: Khairul WM et al., Density functional theory (DFT) calculations, synthesis and electronic properties of alkoxylated-chalcone additive in enhancing the performance of CMC-based solid biopolymer electrolyte, International Journal of Hydrogen Energy, https://doi.org/10.1016/j.ijhydene.2022.06.125

received if not otherwise specified. The spectra and data obtained for infra-red (IR) were performed using PerkinElmer Spectrum 100 Fourier Transform Infrared Spectrometer on KBr pellets within the spectral range of 4000–400 cm^{-1}. The NMR spectra were recorded on a Bruker Avance III 400 Spectrometer at 298K using deuterated chloroform ($CDCl_3$) as solvent and tetramethylsilane (TMS) as an internal standard in the range between δ_H 0–15 ppm for ^1H NMR and δ_C 0–200 ppm for ^{13}C NMR. UV–Vis spectra were recorded by using Spectrophotometer Shimadzu UV-1601PC in cuvette (1 cm^3) with sample concentration of 0.01 mM in dichloromethane. Thermal stability of the titled compound was investigated via Thermogravimetric analysis (TGA) which were carried out on a Perkin–Elmer TGA Analyzer under nitrogen atmosphere.

Computational details

For a supportive evidence to the experimental interpretations, the density functional theory (DFT) calculations were executed by Gaussian 09 software package using Hybrid exchange correlation functional Becke-3-parameters Lee-Yang-Parr (B3LYP) with a polarized 6-31G (d,p) basis set. At first, the optimized geometry of the titled compound according to the energy minima was attained through the same basis set. Subsequently, the optimized structural parameters were used to calculate the vibrational normal mode wavenumber. In our calculation, the compute B3LYP/6-31G (d, p) frequencies scaling factor of 0.9613 has to be used for obtaining a considerably better agreement with experimental data due to the DFT hybrid B3LYP functional method tends to overestimate the fundamental modes [36]. On top of that, to calculate the optical absorption associated with the electronic transition of additive, the absorption and excitation energies wavelengths were performed using time dependent density functional theory (TD-DFT). Their physical properties of electronic characteristics such as E_{HOMO}, E_{LUMO}, HOMO-LUMO gap, ionization potential (IP), electron affinity (EA), and global chemical reactivity descriptors (GCRD) were also calculated. The frontier molecular orbitals (FMO), molecular electrostatic potential (MEP), HOMO and LUMO surface are visualized with Gauss-View 05 program.

Synthetic work

Synthetic pathway of 4-heptyloxyacetophenone (1)

Synthetic experimental details with regards to the preparation of precursor, 4-heptyloxyacetophenone previously has been reported in literature [37] via Williamson alkylation. Despite of the availability of promising method, several modifications have been made in this work to increase the yield and purity of the precursor. 4-Hydroxyacetophenone (0.14 g, 1 mM), heptyl bromide (0.18 g, 1 mM) including K_2CO_3, potassium carbonate (0.40 g, 3 mM), were added into 250 mL 2-neck round bottom flask with 50 mL of dimethylformamide (DMF). The reaction mixture was heated at 60 °C with constant stirring for overnight (*ca.* 12 h). Adjudged completion via thin layer chromatography (TLC), the reaction mixture was allowed to cool to room temperature, then poured into 50 mL water prior organic extraction using n-hexane (2 × 50 mL). The organic portion collected was separated and washed with 1 M aqueous NaOH (20 mL) and then neutralised using aqueous 1 M HCl (20 mL). The organic layer obtained was dried over anhydrous Na_2SO_4 and it was taken to dryness by using rotary evaporator to yield colourless liquid of the title product of 4-heptyloxyacetophenone (**1**). Scheme 1 illustrates the synthetic pathway to synthesis **1**. The confirmation of compound was carried out using FT-IR (KBr, cm^{-1}) in which ν(C–H aliphatic) 2928-2868 cm^{-1}; ν(C=O) 1673 cm^{-1}; ν(C=C) 1603 cm^{-1}. While in ^1H NMR (400.11 MHz, $CDCl_3$): δ 0.82 (t, J = 7.0 Hz, 3H, CH_3); 1.35–1.77 (m, 10H, CH_2); 3.94 (t, J = 7 Hz, 2H, OCH_2); 6.86(pseudo-d, $^3J_{HH}$ = 9 Hz, 2H, Ar–H); 7.84 (pseudo-d, $^3J_{HH}$ = 9 Hz, 2H, Ar–H). ^{13}C NMR (100.61 MHz, $CDCl_3$): δ 13.04 (s, CH_3); 21.57 (s, CH_3) 24.92, 25.28, 28.00, 28.09, 30.73 (5 × s, CH_2); 67.27 (s, CH_2–O); 113.13, 129.12, 129.56, 162.13 (4 × s, Ar–H); 195.78 (s, C=O).

Synthesis of alkoxy-substituted chalcone additive

The preparation of the additive was accomplished via Claisen-Schmidt condensation reaction through equimolar ratio of *para*-nitrobenzaldehyde (0.15g, 1 mM) and **1** (0.23 g, 1 mM), was charged in ethanol (50 mL) in the presence of 15% NaOH solution (approximately 10 mL) as catalyst. The mixture was put at reflux with vigorously stirring for approximately 7 h and the progress was monitored by thin layer chromatography (TLC) (hexane: ethyl acetate) (4:1). Once the reaction was adjudged completion, aqueous 3 M hydrochloric acid (HCl) (5 mL) was carefully added dropwise into the reaction and poured into a beaker containing some crushed ice cubes. The precipitate formed was filtered and recrystallized from acetonitrile to afford corresponding targeted title compound as depicted in Scheme 2 in the form of brick-red solids. FT-IR (KBr, cm^{-1}): ν(C–H aliphatic) 2925-2856 cm^{-1}; ν(C=O) 1654 cm^{-1}; ν(C=C) 1602 cm^{-1}; ν(C–O) 1179 cm^{-1}.^1H NMR (400.11 MHz, $CDCl_3$): δ 0.83 (t, J = 7.0 Hz, 3H, CH_3); 1.35–1.77 (m, 10H, CH_2); 3.98 (t, J = 7 Hz, 2H, OCH_2); 6.92 (pseudo-d, $^3J_{HH}$ = 9 Hz, 2H, Ar–H); 7.71 (pseudo-d, $^3J_{HH}$ = 9 Hz, 2H, Ar–H); 7.60 (d, 1H, J = 16 Hz, β-H); 7.75 (d, 1H, J = 16 Hz, α-H); 7.96 (pseudo-d, $^3J_{HH}$ = 9 Hz, 2H, Ar–H); 8.18 (pseudo-d, $^3J_{HH}$ = 9 Hz, 2H, Ar–H). ^{13}C NMR (100.61 MHz, $CDCl_3$): δ 13.05 (s, CH_3); 21.57, 24.92, 25.28, 28.00, 28.08 (5 × s, CH_2); 67.39 (s, CH_2–O); 113.13, 123.17, 124.70, 127.80, 129.96, (4 × s, Ar–H); 129.21, 140.34 (2 x s, C=C); 147.41 (s, NO_2), 162.13 (s, C–O); 186.71 (s, C=O).

Preparation of SBE containing alkoxy-chalcone additive

Carboxymethyl cellulose (CMC) (2.0g), was obtained from standard commercial supplier Across Organic Co. Dissolved in 16 wt.% of NH_4Cl in 100 mL of distilled water and stirred constantly until complete dissolution of the salt. The quantity of ammonium chloride was fixed to CMC-NH_4Cl at the highest conductivity as testified and acknowledged in previous occasion [38] as reference in this system before adding our synthesized additive. Whilst, in another beaker, various contents of weight percent (0–8 wt. %) of the synthesized alkoxylated-chalcone was dissolved with suitable solvent and carefully added drop by drop at 30 drops/min rate using a Pasteur pipette into a solution of CMC-NH_4Cl with constant stirring for homogenous dissolution formation. The mixture was casted into Petri dish and heated in an oven at constant temperature of 60 °C for *ca.* 42 h for the formation of film. Subsequently, the

Please cite this article as: Khairul WM et al., Density functional theory (DFT) calculations, synthesis and electronic properties of alkoxylated-chalcone additive in enhancing the performance of CMC-based solid biopolymer electrolyte, International Journal of Hydrogen Energy, https://doi.org/10.1016/j.ijhydene.2022.06.125

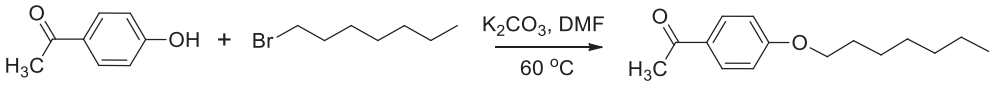

Scheme 1 – Synthetic approach for the preparation of 4-heptyloxybenzaldehye (1).

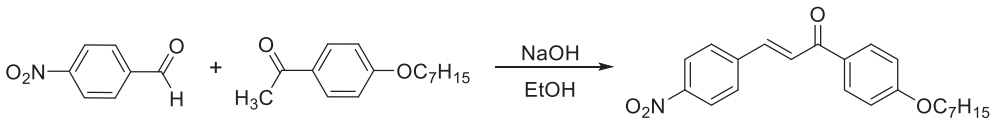

Scheme 2 – Synthetic pathway for the preparation of additive.

films were transferred in a desiccator containing silica gels for further drying process. The summary of the composition and designation of electrolyte in presence of alkoxylated-chalcone additive in CMC-NH_4Cl SBEs are depicted in Table 1. Fig. 1 represents the flow of the SBE preparation in this work.

SBE characterization

Electrical impedance spectroscopy (EIS)

Electrical conductivity measurement was carried out using HIOKI 3532-50 LCR High-tester within the frequency of 50 Hz to 1 MHz and tested at room temperature 303K. The SBE sample was cut into a fitting size of small discs with diameter 2 cm and sandwiched between two stainless steel blocking electrodes of a conductivity cell which connected to LCR tester. The bulk resistance (R_b) value attained from the graph of negative imaginary impedance (Z_i) against real part of impedance (Z_r) known as Cole–Cole plot. The ionic conductivity (σ) of the sample was calculated using the following equation:

$$\sigma = t / R_b a \quad (1)$$

From the equation, t (cm) is the thickness of film, R_b (ohm) is bulk resistance of film and A (cm^2) is the cross-sectional area of electrode-electrolyte which is 3.142 cm^2.

Results and discussion

Spectroscopic study

Both experimental and calculated infrared spectra of the additive revealed all the expected IR characteristics bands of interest namely ν(C–H), ν(C=O), ν(C=C), ν(C–O), υ(N–H), υ(C–N) and $\upsilon(NO_2)$ ranging from weak to strong intensities. The C–H stretching frequency of aromatic and aliphatic are commonly detected in the range of 3100–3000 cm^{-1} and 2850-3000 cm^{-1} [39,40]. In this study, aromatic C–H stretching vibrations of phenyl rings were assigned at 3195, 3109 cm^{-1} and 3075 in FT-IR spectra and were calculated at 3120, 3106 and 3075 cm^{-1}. The observe band in the range of 2856 cm^{-1} to 2925 cm^{-1} corresponded to the ν(C–H aliphatic) stretching vibrations within the alkoxy chains whilst the theoretical values are in the region of 2891–2991 cm^{-1}. The ν(C=O) stretching vibration detected at lower wavenumber at 1655 cm^{-1} (experimental) and 1673 cm^{-1} (theoretical) with strong intensity. The occurrence due to the π-electrons delocalization between α and β carbons which reduced the C=O order and consequently increase the bond order between the carbonyl carbon and α carbon atom [41]. In this sense, the carbonyl group vibration dependent on the strength of bonding, lone pairs of electrons on the oxygen atoms and inductive effect. The characteristics of the conjugation at double bond (C=C) of ethylene moiety character is shown by chalcone derivative at 1603 cm^{-1} and C=C aromatic was found at the wavenumber of 1467 cm^{-1}. The summarized data for observed and calculated frequencies along with their probable assignment are presented in supplementary data (Table S1) and spectra are depicted in Figs. S1–S2.

^1H and ^{13}C nuclear magnetic resonance (NMR) analysis of additive

The ^1H NMR spectrum of the additive revealed the present $-CH_3$ proton at δ_H 0.83 ppm as triplet resonance while CH_2 (aliphatic) group was observed as multiplet overlapping resonance at the upfield region δ_H 1.26–1.78 ppm. The chemical shift of R–OCH_2 moiety was detected at deshielded region at δ_H 3.98 ppm as triplet resonance. The aromatic protons were positioned in the higher chemical shift in the range of δ_H 6.92–8.18 ppm as *pseudo*-doublet resonances due to the

Table 1 – The composition and designation scheme of SBEs in this work.

Designation	Formulation				
	CMC (g)	NH_4Cl (wt.%)	NH_4Cl (g)	Additive (wt.%)	Additive (g)
A0	2	0	0	0	0
A16	2	16	0.381	0	0
B1	2	16	0.381	2	0.05
B2	2	16	0.381	4	0.10
B6	2	16	0.381	6	0.15
B8	2	16	0.381	8	0.20

Please cite this article as: Khairul WM et al., Density functional theory (DFT) calculations, synthesis and electronic properties of alkoxylated-chalcone additive in enhancing the performance of CMC-based solid biopolymer electrolyte, International Journal of Hydrogen Energy, https://doi.org/10.1016/j.ijhydene.2022.06.125

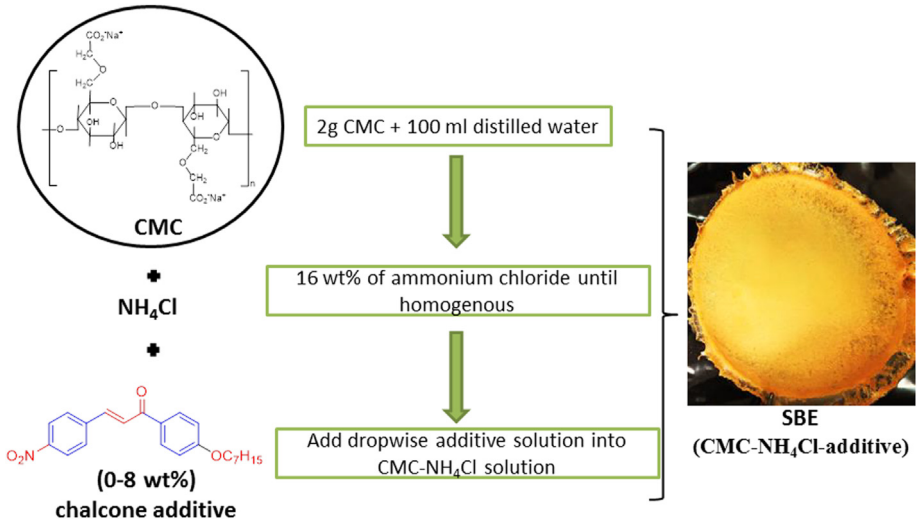

Fig. 1 – The preparation of CMC-NH_4Cl-additive SBE system.

existence of electronegative atoms attached to the phenyl ring. At higher chemical shift of δ_H 7.56–7.60 ppm and δ_H 7.71–7.75 ppm, there are existence of two doublets in this overlapped region with higher value of coupling constants (J = 16 Hz) attributed that ethylene moiety in the enone linkage is in the *E*-geometry, which strongly confirms the formation of chalcones as reported in the previous study [42]. In the ^{13}C NMR spectrum, the methyl resonance can be seen at δ_C 13.05 ppm and carbon resonances for alkyl chain length (C_nH_{2n+1}) were identified at around δ_C 21.57–30.73 ppm. Meanwhile, at δ_C 67.39 ppm, the chemical shift for R–CH_2-O- can be observed due to the deshielding effect in the existence of oxygen atom that withdrew some amount of electron density from the alkyl chain attached to the phenyl ring. Parallelly, these observation of these established signals in the ^{13}C NMR spectrum indicates the existence of the alkoxy (-OR) substructure in the designed and its expected chalcone structure. Two sequential signals at δ_C 129.21 ppm and δ_C 147.41 ppm belong to the resonances of C_α and C_β carbon atoms of the α,β-unsaturated carbonyl system in any typical chalcone [43]. The resonances of carbons for phenyl rings were observed in the region δ_C 113.49–16254 ppm, whilst signal detected at δ_C 186.71 ppm was ascribed to the presence of carbonyl (C=O) carbon atom. The spectra of ^1H and ^{13}C NMR of the additive are tabulated in details in Supplementary material 1 (Figs. S3–S4).

UV–visible and electronic properties

The electronic transition spectrum of additive as depicted in Fig. 2 revealed single major principal absorption band which believed arising from several designated chromophores which may include phenyl rings, carbonyl, ethylene as well as NO_2 substituent. In this perspective, the broadness of the absorption spectrum may arise due to a contribution from more than one electronic state to the absorption spectrum. A broad and strong intensity absorption band of maximum wavelength (λ_{max}) centred at λ_{max} 312 nm whilst the cut-off wavelength (λ_{edge}) found at 395 nm attributed from overlapping mixed transitions of $\pi\rightarrow\pi^*$- and $n\rightarrow\pi^*$. The $\pi\rightarrow\pi^*$ transition arises from ethylene portion of the molecule and contributed by π-bonding orbitals of the phenyl rings while $n\rightarrow\pi^*$ transition is expected to be contributed by from carbonyl moiety and $-NO_2$ auxochrome. Subsequently, the optical energy band gap (E_g) was calculated using Eq. (2) which expressed in eV. According to formula of $E_{gap} = hc/\lambda_{edge}$, the E_g value of additive is exhibited 3.14 eV which lies in semiconductor properties.

$$E_g^{opt}\ (eV) = 1240 / \lambda_{edge} \quad (2)$$

The nature of excited states and charge transfer properties that involved in electronic absorption processes, the electronic transitions and energy values of HOMO and LUMO of the additive was calculated using density functional theory (DFT). The time dependent-DFT approach employing B3LYP functional and 6-31G (d,p) basis set in solvent effects (dichloromethane) through Integral Equation Formalism Polarizable Continuum Model (IEF-PCM) were computed. In these sense, the experimental UV spectra were taken as reference to validate the electronic absorption spectra in theoretical calculations. Both experimental and simulated spectrum showed good agreement with one intense band centred at 395 nm (experimental) and 407 nm (simulated). The calculated absorption maxima values show notable red shift compared to experimental absorption as illustrated in Fig. 3. The slightly different of absorption maxima ascribed due to the solvation effect led generally to a red shift in the main transition wavelengths to stabilize molecular orbitals in the excited state. The major peak from simulated spectrum represents contributions from electronic transition from HOMO→LUMO orbitals [44]. The calculated wavelength (λ) of electronic excitation energies at various energy levels, oscillator strength (f), energy gap with major contributors are listed in Table 2.

Additionally, the HOMO-LUMO level of the targeted compound is illustrated in Fig. 4 which obtained and derived from quantum chemical calculations. Apparently, the electron cloud of the HOMO level is mainly located on the spacer containing the substituents of oxygen and phenyl, whereas

Please cite this article as: Khairul WM et al., Density functional theory (DFT) calculations, synthesis and electronic properties of alkoxylated-chalcone additive in enhancing the performance of CMC-based solid biopolymer electrolyte, International Journal of Hydrogen Energy, https://doi.org/10.1016/j.ijhydene.2022.06.125

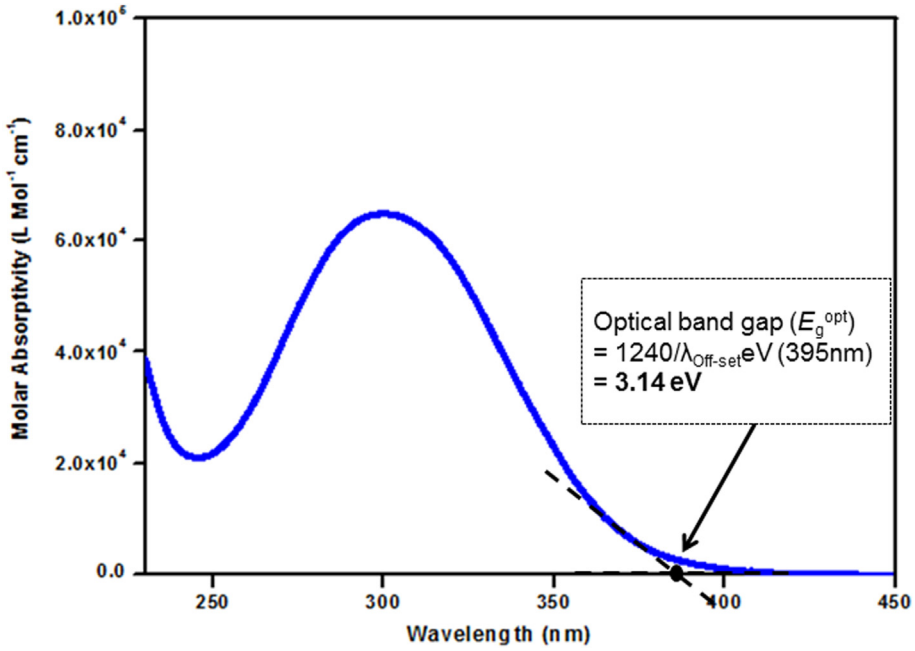

Fig. 2 – UV–Vis absorption spectrum and respective band gap energy estimation for the additive.

the LUMO level is dominated by orbitals from the nitro and chalcone moieties. Generally, such electron distribution explains clearly on the investigated molecule with a fundamental aspects of intramolecular charge transfer property, which is consistent and parallel with the experimental spectroscopic data. In addition, this minimal overlapping of HOMO-LUMO also afforded with smaller energy for photoexcitation and relaxation, thus in this particular molecule, its calculated theoretical band gap energy (E_g) was as 2.89 eV which lies in the typical band gap range of functional organic semiconducting materials.

Further, global reactivity descriptors parameters assist to elucidate the chemical reactivity, kinetic stability, chemical hardness-softness of a molecule and electronic properties of the organic semiconductor application. In this respects, ionization potential (I), electron affinity (A), global hardness (η), chemical potential (μ), electrophilicity index (ω), global softness (S), electronegativity (χ) are calculated using the basis of

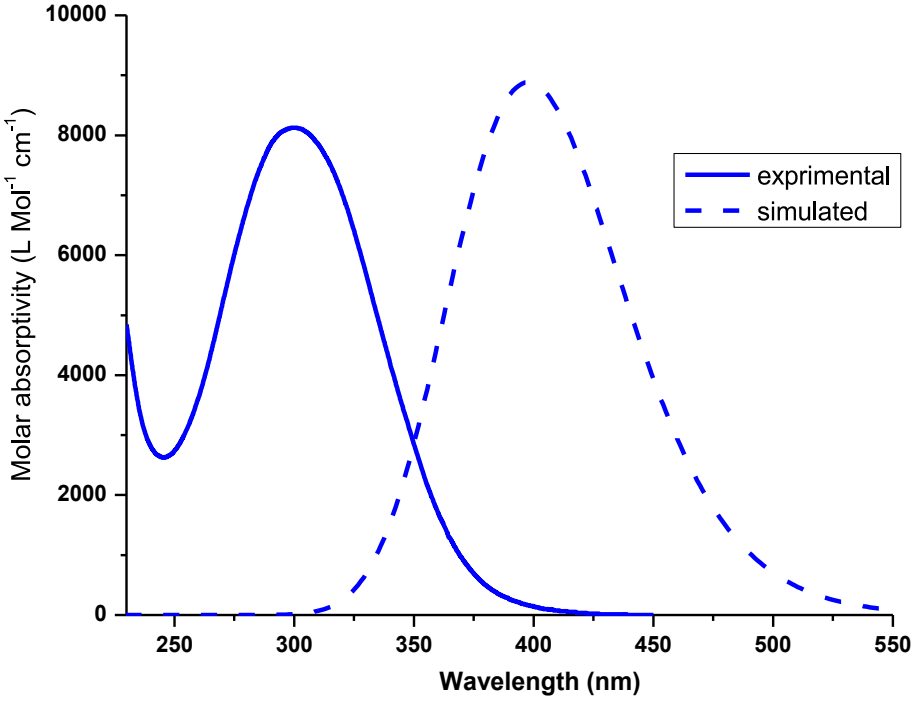

Fig. 3 – Experimental (straight line) and simulated (dashed line) for UV–Vis spectra of the additive.

Please cite this article as: Khairul WM et al., Density functional theory (DFT) calculations, synthesis and electronic properties of alkoxylated-chalcone additive in enhancing the performance of CMC-based solid biopolymer electrolyte, International Journal of Hydrogen Energy, https://doi.org/10.1016/j.ijhydene.2022.06.125

Table 2 – The excitation energy, experimental and calculated absorption wavelength, major contribution and corresponding oscillator strengths (*f*) of additive.

Excited state	Wavelength (nm)		Oscillator strength, *f*	Excitation energies (ΔE, eV)	Excitation transitions
	Experimental	Calculated			
$S_0 \rightarrow S_1$	395	407 397	0.2194	3.1164	HOMO→LUMO (99%) HOMO→LUMO+1 (53%)

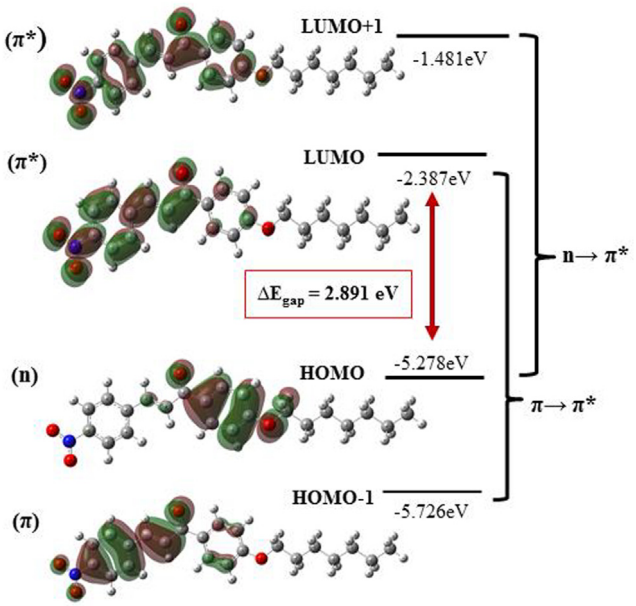

Fig. 4 – Molecular orbital involved in the electronic transition of the additive.

energy values of frontier molecular orbitals (FMO) following the suggestion by Koopman's theorem [45,46]:

$$\text{Ionization potential, } I = -E_{HOMO} \quad (3)$$

$$\text{Electron affinity, } A = -E_{LUMO} \quad (4)$$

$$\text{Global hardness, } \eta = \frac{I-A}{2} \quad (5)$$

$$\text{Chemical potential, } \mu = \frac{-(I+A)}{2} \quad (6)$$

$$\text{Electrophilicity index, } \omega = \frac{\mu^2}{2\eta} \quad (7)$$

$$\text{Global Softness, } S = \frac{1}{\eta} \quad (8)$$

$$\text{Electronegativity, } \chi = \frac{I+A}{2} \quad (9)$$

The calculated values of all the related parameters are summarized in Table 3. A HOMO value indicates a tendency of the molecule to donate electrons to appropriate acceptor while the values of LUMO energy indicate the possibility to accept electrons. The outcome reveals that HOMO–LUMO energy gap is directly proportional to the low chemical hardness for this additive system. From the previous reported literature [47,48], addition of low chemical hardness additive reduces the hardness of the biopolymer and enhancing the piezoelectric property.

Besides, molecular electrostatic potential (MEP) mapping has been employed primarily for recognition of the molecular interactions, forecast of relative locations for nucleophilic and electrophilic attacks which provide the information of preferred sites for hydrogen bonds. The negative region of MEP related to an attraction of the proton by the aggregation of electron density in the molecule (shades in red) are preferred site for nucleophilic, whereas the positive region of MEP corresponds to a repulsion of the proton by the atomic nuclei (shade of blue) and preferred site for electrophilic. The obtained MEP plots of additive is visualized in Fig. 5.

According to the MEP maps in Fig. 5, it is evident that negative (red) region localized on the oxygen and nitrogen atom in alkoxy and nitro units while the positive (blue) region is observed over the hydrogen of aromatic rings and alkoxy chain which indicate electrophilic attraction. Additionally, the green region has spread at the MEP surface which confirms the existence of an intermolecular interaction in the system.

Thermal analysis

Thermal behaviour of the synthesized additive exhibited good stability up to *ca.* 280 °C and no weight loss occurred below 100 °C which evidence there was no entrapped of water molecule or solvent presence in the sample. The TGA/DTG curve revealed a single degradation step took place at around 276–280 °C (T_{onset}) and ended at around 350–356 °C (T_{offset}) with sharp endothermic DTG as portrayed in Fig. 6. This occurrence implies the decomposition of all chalcone moieties including alkoxy and nitro substituents into volatile gaseous products. During the decomposition of this stage, the total weight loss was 98.5% with maximum degradation (T_{max}) occurred at 335 °C. The incorporation of long alkoxy chain in chalcone moiety has aided further stabilization by π-stacking between adjacent aromatic portion, carbonyl and ethylene moieties as

Table 3 – Calculated global reactivity parameter for alkoxylated-chalcone, the additive.

Parameter	Value (eV)
Ionization potential (*I*)	5.278
Electron affinity (*A*)	2.387
Global hardness (η)	1.445
Chemical potential (μ)	−3.833
Electrophilicity index (ω)	5.0824
Global Softness (*S*)	0.730
Electronegativity (χ)	3.054

Please cite this article as: Khairul WM et al., Density functional theory (DFT) calculations, synthesis and electronic properties of alkoxylated-chalcone additive in enhancing the performance of CMC-based solid biopolymer electrolyte, International Journal of Hydrogen Energy, https://doi.org/10.1016/j.ijhydene.2022.06.125

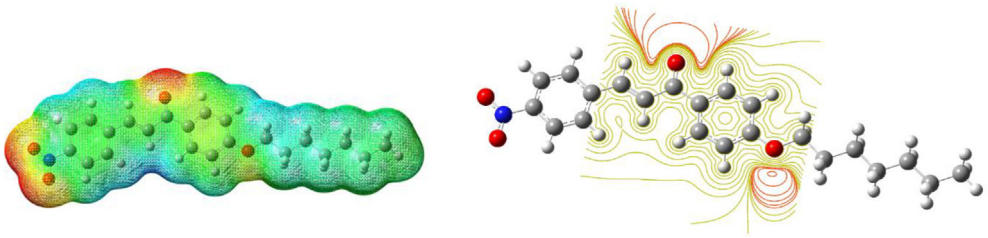

Fig. 5 – Molecular surface of synthesize additive.

is in good agreement with previously reported literatures [40,49]. From thermal behaviour trend of additive, it displayed satisfactory thermal stability at high temperature and it gave good indications to be applied in film fabrication as it exhibits remarkable performance under prolonged thermal stress.

Ionic conductivity study of SPEs at room temperature

The effects of doping salt and the synthesized alkoxylated-chalcone additive on ionic conductivity of pure CMC have been calculated from bulk resistance (R_b) of the SBEs obtained by the intercepts of the ac impedance curves at room temperature (303K) and the obtained results are listed in Table 4. The noticeable increment of ionic conductivity from 2.03×10^{-7} Scm^{-1} to 1.69×10^{-3} Scm^{-1} upon the addition of 16 wt.% of NH_4Cl salt into CMC was comparative as found by Ahmad & Isa, 2016 [38]. Thus, CMC-NH_4Cl SPEs has recorded the highest conduction in salted system (16 wt.%) was further carried out to study the influence of synthesized alkoxylated-chalcone additives with the aims to improve the performance of ionic conductivity of the SPEs system.

In this sense, the value of ionic conductivity increases monotonically with incorporation of organic additive of synthesized alkoxylated-chalcone and reaches maximum value of 2.30×10^{-2} Scm^{-1} for sample **B6** containing 6 wt.% of additives. The conductivity increases gradually with increasing wt.% of additive composition and this implying the effectiveness of the synthesized chalcone additive in dissociating doping salt (NH_4Cl) in CMC matrix. Hence, there will be more protons (H^+) are supplied [50] due to the dissociation of the doping salt at which ion hopping and exchange can take place leading to an enhancement in conductivity [51]. Nevertheless, the electrical conductivity decreases after 8 wt.% of the additive is added due to optimum concentration of additive has been achieved and lead to greater tendency towards

Table 4 – Designation of the Thickness, Bulk resistance (Ω) and Conductivity (σ) values at room temperature of SPEs system.

Designation	Thickness, t (cm)	Bulk Resistance, R_b (Ω)	Conductivity, σ (S/cm)
A0	0.015	23,500.00	2.03×10^{-7}
A16	0.015	2.82	1.69×10^{-3}
B1	0.090	1.86	1.54×10^{-2}
B2	0.020	1.61	1.80×10^{-2}
B6	0.060	0.83	2.30×10^{-2}
B8	0.096	1.77	1.73×10^{-2}

Composition of additive (wt.%): **A0** = 0; **A16** = 0; **B1** = 2; **B2** = 4; **B6** = 6; **B8** = 8.

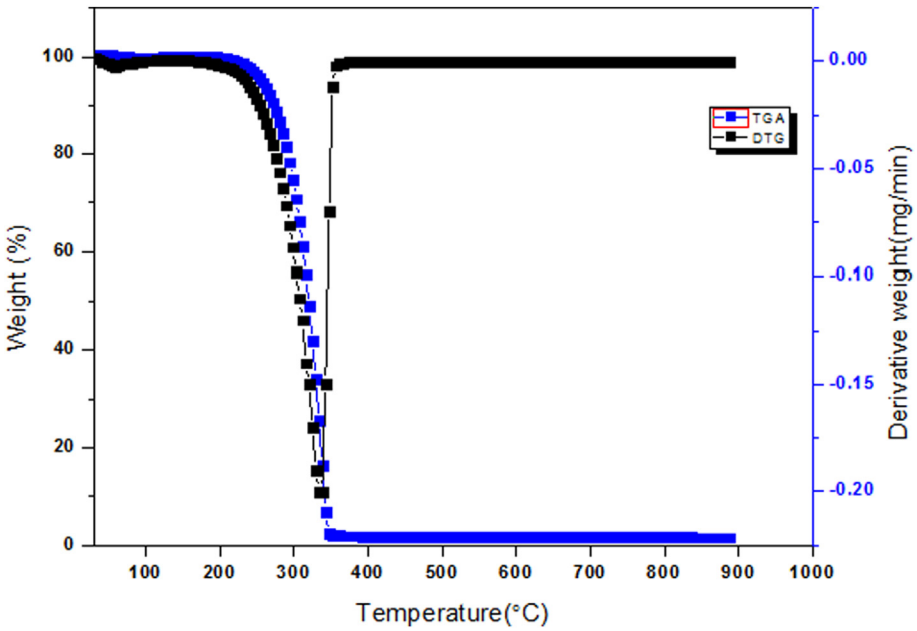

Fig. 6 – TGA/DTG thermogram of the additive.

Please cite this article as: Khairul WM et al., Density functional theory (DFT) calculations, synthesis and electronic properties of alkoxylated-chalcone additive in enhancing the performance of CMC-based solid biopolymer electrolyte, International Journal of Hydrogen Energy, https://doi.org/10.1016/j.ijhydene.2022.06.125

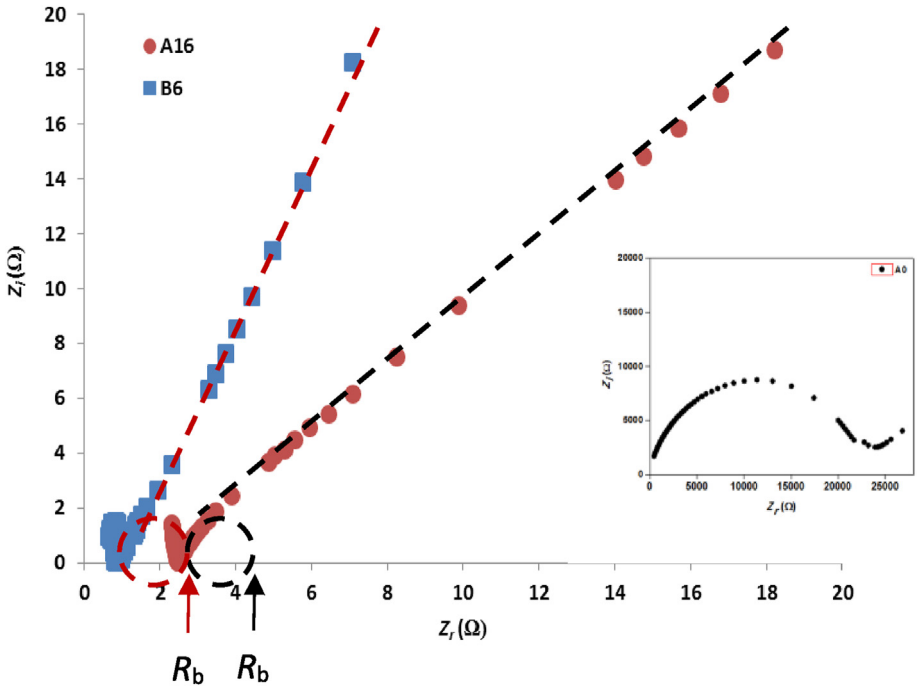

Fig. 7 – Cole-cole plot of the SBEs system at room temperature.

sample aggregation hence increase the degree of crystallinity in the electrolyte system.

Fig. 7 reveals the Cole–Cole plot of the highest conducting SBEs for **A16** and **B6** at ambient temperature (303 K) and inset figure shows the plot for pure **A0** film. The semicircle in **A0** at high frequency region inferring the CMC biopolymer is partially bulk resistance and bulk capacitance [52]. Notably, the semi-circle and bulk resistance (R_b) decrease upon the addition of salt and further decrease with incorporation of chalcone additive until 6 wt%. Resulted the increment of ionic conductivity in the SPE system. The ac impedance plots of **A16** and **B6** exhibited spike in the low-frequency region is inferred that the SBE sample is in resistive nature.

Conclusions

The role and performance of alkoxylated-chalcone based compound as the additive in new proton conducting solid bio-polymer electrolytes based on CMC and NH_4Cl has been successfully synthesized, characterized and prepared using solution casting techniques. The synthesized alkoxylated-chalcone additive possesses thermal stability at high temperature and exhibited highest conductivity of 2.3×10^{-2} Scm^{-1} for the SBE system containing 6 wt.% of the additive at ambient temperature. Therefore, the findings from this study have proven that, even with a little change in properties of conductivity upon an addition of the synthesized chalcone compound as additive of this molecular candidate would provide an improvement in term of ideally effective and recognisable charge transport pathways in SBEs leading to enhancement in any potential electrochemical devices.

CRediT authorship contribution statement

Wan M. Khairul: Conceptualization, Supervision of synthetic chemistry and Characterization, Reviewing, Editing, Revising and Manuscript approval, funding acquisition. **Janice Roria Joni:** Data Collection, Methodology, Experimental Work, Computational Analysis and Other Related Data Analyses. **Rafizah Rahamathullah:** Methodology, Data curation, Visualization, Computational Analysis, Writing-original draft. **M.I.N Isa:** Contributed in Supervision of SPE analysis, Editing and Reviewing the Manuscript.

Declaration of competing interest

The authors declare that they have no known competing financial interests or personal relationships that could have appeared to influence the work reported in this paper.

Acknowledgements

The authors would like to express gratitude to the Organisation for the Prohibition of Chemical Weapons (OPCW) (Grant numbers: 53309 (UMT's referral code), OPCW's Project Account No: L/ICA/ICB/217568/18) for research grant support, and

Universiti Malaysia Terengganu (UMT) for research supports, facilities and research aids.

Appendix A. Supplementary data

Supplementary data to this article can be found online at https://doi.org/10.1016/j.ijhydene.2022.06.125.

REFERENCES

[1] Ahmad S, Nawaz T, Ali A, Orhan MF, Samreen A, Kannan AM. An overview of proton exchange membranes for fuel cells: materials and manufacturing. Int J Hydrogen Energy 2022;47:19086–131.

[2] Liu X, Sun Y, Tong Y, Wang X, Zheng J, Wu Y, Li H, Niu L, Hou Y. Exploration in materials, electrolytes and performance towards metal ion (Li, Na, K, Zn and Mg)-based hybrid capacitors: a review. Nano Energy 2021;86:106070.

[3] Zhang X, Meng J, Wang X, Xiao Z, Wu P, Mai L. Comprehensive insights into electrolytes and solid electrolyte interfaces in potassium-ion batteries. Energy Storage Mater 2021;38:30–49.

[4] Guo S, Qin L, Zhang T, Zhou M, Zhou J, Fang G, Liang S. Fundamentals and perspectives of electrolyte additives for aqueous zinc-ion batteries. Energy Storage Mater 2021;34:545–62.

[5] Wong CY, Wong WY, Ramya K, Khalid M, Loh KS, Daud WRW, Lim KL, Walvekar R, Kadhum AAH. Additives in proton exchange membranes for low-and high-temperature fuel cell applications: a review. Int J Hydrogen Energy 2019;44:6116–35.

[6] Daeneke T, Kwon TH, Holmes AB, Duffy NW, Bach U, Spiccia L. High-efficiency dye-sensitized solar cells with ferrocene-based electrolytes. Nat Chem 2011;3:211.

[7] Hosseini S, Xu TH, Soltani SM, Ko TE, Lin YJ, Li YY. The efficient acetoxy-group-based additives in protecting of anode in the rechargeable aluminium-air batteries. Int J Hydrogen Energy 2022;47:501–16.

[8] Xu N, Shi J, Liu G, Yang X, Zheng J, Zhang Z, Yang Y. Research progress of fluorine-containing electrolyte additives for lithium ion batteries. J Power Sour Adv 2021;7:100043.

[9] Abisharani JM, Balamurugan S, Thomas A, Devikala S, Arthanareeswari M, Ganesan S, Prakash M. Incorporation of organic additives with electron rich donors (N, O, S) in gelatin gel polymer electrolyte for dye sensitized solar cells. Sol Energy 2021;218:552–62.

[10] Ganesan S, Mathew V, Paul BJ, Maruthamuthu P, Suthanthiraraj SA. Influence of organic nitrogenous compounds phenothiazine and diphenyl amine in poly (vinylidene fluoride) blended with poly (ethylene oxide) polymer electrolyte in dye-sensitized solar cells. Electrochim Acta 2013;102:219–24.

[11] Saidi NM, Farhana NK, Ramesh S, Ramesh K. Influence of different concentrations of 4-tert-butyl-pyridine in a gel polymer electrolyte towards improved performance of Dye-Sensitized Solar Cells (DSSC). Sol Energy 2021;216:111–9.

[12] Karthika P, Ganesan S, Thomas A, Rani TMS, Prakash M. Influence of synthesized thiourea derivatives as a prolific additive with tris (1,10-phenanthroline) cobalt (II/III) bis/tris (hexafluorophosphate)/hydroxypropyl cellulose gel polymer electrolytes on dye-sensitized solar cells. Electrochim Acta 2019;298:237–47.

[13] Chatterjee K, Pathak AD, Sahu KK, Singh AK. New thiourea-based ionic liquid as an electrolyte additive to improve cell safety and enhance electrochemical performance in lithium-ion batteries. ACS Omega 2020;5(27):16681–9.

[14] Nadiah NS, Omar FS, Numan A, Mahipal YK, Ramesh S, Ramesh K. Influence of acrylic acid on ethylene carbonate/dimethyl carbonate based liquid electrolyte and its supercapacitor application. Int J Hydrogen Energy 2017;42:30683–90.

[15] Xia L, Xia Y, Liu Z. Thiophene derivatives as novel functional additives for high-voltage $LiCoO_2$ operations in lithium ion batteries. Electrochim Acta 2015;151:429–36.

[16] Wang F, Li L, Yang X, You J, Xu Y, Wang H, Ma Y, Gao G. Influence of additives in a PVDF-based solid polymer electrolyte on conductivity and Li-ion battery performance. Sustain Energy Fuels 2018;2(2):492–8.

[17] Yang Y, Zhang Z, Gao J, Pan D, Yuan B, Guo X, Huang G. Metal-organic materials as efficient additives in polymer electrolytes for quasi-solid-state dye-sensitized solar cells. J Alloys Compd 2017;726:1286–94.

[18] Cao L, Skyllas-Kazacos M, Menictas C, Noack J. A review of electrolyte additives and impurities in vanadium redox flow batteries. J Energy Chem 2018;27(5):1269–91.

[19] Shaari N, Kamarudin SK. Recent advances in additive-enhanced polymer electrolyte membrane properties in fuel cell applications: an overview. Int J Energy Res 2019;43(7):2756–94.

[20] Selvam R, Subramanian K. Benzimidazole-indole-chalcone connected methacrylate-based side chain D-π-A polymer and its application in organic photovoltaics. J Polym Sci: Polym Chem 2017;55(6):997–1007.

[21] Shehzad RA, Muhammad S, Chaudhry AR, Ito S, Iqbal J, Khalid M, Aloui Z, Xu HL. Electro-optical and charge transport properties of chalcone derivatives using a dual approach from molecule to material level simulations. Comput Theor Chem 2021;1203:113349.

[22] Makhlouf MM, Radwan AS, Ghazal B. Experimental and DFT insights into molecular structure and optical properties of new chalcones as promising photosensitizers towards solar cell applications. Appl Surf Sci 2018;452:337–51.

[23] Çelik T, Coşkun MF. Dielectric and thermal properties of the methacrylate polymer bearing chalcone side group. J Mol Struct 2018;1157:239–46.

[24] Yan BL, Sun R, Ge JF, Wang D, Li H, Lu JM. Electronic memory devices based on the chalcone with negative electrostatic potential regions. Mater Chem Phys 2013;142(1):363–9.

[25] Sarkı G, Kantekin H, Yalazan H, Kahriman N, Biyiklioglu Z, Serdaroğlu V. Synthesis, characterization and electrochemical studies of metal-free and metallophthalocyanines containing two different chalcone units substituted on peripherally positions. J Mol Struct 2019;1196:592–603.

[26] Ahmad S, Nawaz T, Ali A, Orhan MF, Samreen A, Kannan AM. An overview of proton exchange membranes for fuel cells: materials and manufacturing. Int J Hydrogen Energy 2022;47(44):19086–131.

[27] Singh R, Polu AR, Bhattacharya B, Rhee HW, Varlikli C, Singh PK. Perspectives for solid biopolymer electrolytes in dye sensitized solar cell and battery application. Renew Sustain Energy Rev 2016;65:1098–117.

[28] Irfan M, Atif M, Yang Z, Zhang W. Recent advances in high performance conducting solid polymer electrolytes for lithium-ion batteries. J Power Sources 2021;486:229378.

[29] Torres FG, De-la-Torre GE. Algal-based polysaccharides as polymer electrolytes in modern electrochemical energy conversion and storage systems: a review. Carbohydr Polym Technol Appl 2021;2:100023.

[30] Zainuddin NK, Rasali NMJ, Mazuki NF, Saadiah MA, Samsudin AS. Investigation on favourable ionic conduction based on CMC-K carrageenan proton conducting hybrid solid

bio-polymer electrolytes for applications in EDLC. Int J Hydrogen Energy 2020;45(15):8727–41.
[31] Saadiah MA, Nagao Y, Samsudin AS. Enhancement on protonation (H^+) with incorporation of flexible ethylene carbonate in CMC–PVA–30 wt% NH_4NO_3 film. Int J Hydrogen Energy 2021;46(33):17231–45.
[32] Gupta S, Varshney PK. Effect of plasticizer on the conductivity of carboxymethyl cellulose-based solid polymer electrolyte. Polym Bull 2019;76(12):6169–78.
[33] Foran G, Mankovsky D, Verdier N, Lepage D, Prébé A, Aymé-Perrot D, Dollé M. The impact of absorbed solvent on the performance of solid polymer electrolytes for use in solid-state lithium batteries. iScience 2020:101597.
[34] Ambika C, Karuppasamy K, Vikraman D, Lee JY, Regu T, Raj TAB, Prasanna K, Kim HS. Effect of dimethyl carbonate (DMC) on the electrochemical and cycling properties of solid polymer electrolytes (PVP-MSA) and its application for proton batteries. Solid State Ionics 2018;321:106–14.
[35] Wong CY, Wong WY, Ramya K, Khalid M, Loh KS, Daud WRW, Lim KL, Walvekar R, Kadhum AAH. Additives in proton exchange membranes for low-and high-temperature fuel cell applications: a review. Int J Hydrogen Energy 2019;44(12):6116–35.
[36] Wong MW. Vibrational frequency prediction using density functional theory. Chem Phys Lett 1996;256(4–5):391–9.
[37] Tantrawong S, Styring P, Goodby JW. Discotic mesomorphism in oxovanadium (IV) complexes possessing four alkyl substituents. J Mater Chem 1993;3:1209–16.
[38] Ahmad NH, Isa MIN. Characterization of un-plasticized and propylene carbonate plasticized carboxymethyl cellulose doped ammonium chloride solid biopolymer electrolytes. Carbohyd polym 2016;137:426–32.
[39] Lima IKC, de Sousa FD, de Morais Bento AJ, Cruz BG, da Silva PT, Bandeira PN, dos Santos HS, Saraiva GD, Barreto ACH, Freire PDTC, Teixeira AMR. Structural and spectroscopic investigation of the chalcones (E)-1-(4-aminophenyl)-3-(4′-ethoxyphenyl)-prop-2-en-1-one and (E)-1-(aminophenyl)-3-(4′-methoxyphenyl)-prop-2-en-1-one. Vib Spectrosc 2020;110:103118.
[40] Daud AI, Khairul WM, Augustine E, Arshad S, Razak IA. Synthesis, spectroscopic, structural elucidation, NLO characteristic and Hirshfeld surface analysis of (E)-1-(4-ethylphenyl)-3-(4-(heptyloxy) phenyl) prop-2-en-1-one: a dual approach of experimental and DFT calculations. J Mol Struct 2019;1194:124–37.
[41] Coskun D, Erkisa M, Ulukaya E, Coskun MF, Ari F. Novel 1-(7-ethoxy-1-benzofuran-2-yl) substituted chalcone derivatives: synthesis, characterization and anticancer activity. Eur J Med Chem 2017;136:212–22.
[42] El-Meligie S, Taher AT, Kamal AM, Youssef A. Design, synthesis and cytotoxic activity of certain novel chalcone analogous compounds. Eur J Med Chem 2017;126:52–60.
[43] Thirunarayanan G, Gopalakrishnan M, Vanangamudi G. IR and NMR spectral studies of 4-bromo-1-naphthyl chalcones-assessment of substituent effects. Spectrochim Acta: Mol Biomol Spectrosc 2007;67(3–4):1106–12.
[44] Saeed A, Shehzadi SA, Bolte M, Franca CA, Erben MF. Interplay between conformation and crystal packing in aryl propargyl ethers: structural and spectroscopic properties of 2-(prop-2-yn-1-yloxy) acene derivatives. ChemistrySelect 2019;4(34):9927–33.
[45] Zhan CG, Nichols JA, Dixon DA. Ionization potential, electron affinity, electronegativity, hardness, and electron excitation energy: molecular properties from density functional theory orbital energies. J Phys Chem A 2003;107(20):4184–95.
[46] Koopmans T. Über die Zuordnung von Wellenfunktionen und Eigenwerten zu den einzelnen Elektronen eines Atoms. Physica 1934;1(1–6):104–13.
[47] Sarkar R, Kundu TK. Density functional theory studies on PVDF/ionic liquid composite systems. J Chem Sci 2018;130(8):1–18.
[48] Shukla V, Gupta AK, Gupta SK. Theoretical studies on structural and optical properties of PEO & NH4SCN based solid polymer elect$_r$olyte. In: AIP conference proceedings. AIP Publishing LLC; 2020, October, 030062. 2269.
[49] Saeed A, Ashraf S, White JM, Soria DB, Franca CA, Erben MF. Synthesis, X-ray crystal structure, thermal behavior and spectroscopic analysis of 1-(1-naphthoyl)-3-(halo-phenyl)-thioureas complemented with quantum chemical calculations. Spectrochim Acta: Mol Biomol Spectrosc 2015;150:409–18.
[50] Hashmi SA, Kumar A, Maurya KK, Chandra S. Proton-conducting polymer electrolyte. I. The polyethylene oxide + NH_4ClO_4 system. J Phys D Appl Phys 1990;23:1307.
[51] Osman Z, Ibrahim ZA, Arof AK. Conductivity enhancement due to ion dissociation in plasticized chitosan based polymer electrolytes. Carbohydr Polym 2001;44:167–73.
[52] Samsudin AS, Khairul WM, Isa MIN. Characterization on the potential of carboxy methylcellulose for application as proton conducting biopolymer electrolytes. J Non-Cryst Solids 2012;358:1104–12.

Please cite this article as: Khairul WM et al., Density functional theory (DFT) calculations, synthesis and electronic properties of alkoxylated-chalcone additive in enhancing the performance of CMC-based solid biopolymer electrolyte, International Journal of Hydrogen Energy, https://doi.org/10.1016/j.ijhydene.2022.06.125